

Development of an inspection robot for small diameter gas distribution mains

Edwin Dertien
University of Twente
CTIT Institute
Enschede, The Netherlands
e.c.dertien@utwente.nl

Stefano Stramigioli
University of Twente
CTIT Institute
Enschede, The Netherlands
s.stramigioli@ieee.org

Kees Pulles
KIWA Gastec B.V.
Apeldoorn, The Netherlands
k.pulles@kiwa.nl

Abstract—This paper discusses the design of a mechanical structure of a miniature pipe inspection robot capable of moving through very small pipes (down to 41 mm inner diameter). The requirement to negotiate bends, T-joints and steep inclinations pose another set of strict design constraints. The proposed robot consists of a modular design (7 modules) with a relatively low number of active degrees of freedom. The system is using a novel clamping mechanism with a series-elastic drive. The design of this mechanism has resulted in a high spreading factor allowing the system to operate in a wide diameter range (63 mm to 125 mm outer diameter). In this paper the mechanical design requirements and control system will be discussed. Preliminary test results will be given.

I. INTRODUCTION

A. Network

The network of gas distribution mains can be divided into a high-pressure (1-8 bar) network for regional distribution and low pressure networks (30 mbar to 100 mbar) for local distribution. This low-pressure net occupies most of the urban area's. Therefore this network has the highest priority regarding risks for public health and safety. Replacement of pipe-lines in an urban area is expensive, so it is important to have accurate data on the locations of leaks or damaged sections. Detailed information on condition of the network and accurate location of leaks is vital for future safe operation. The feasibility and economic potential of the system have been presented at [1].

B. Current methodology for leak searching

Currently, the low pressure distribution nets are mostly inspected by leak survey above ground. This is a labour-intensive process and does not yield any information about layout and quality of the pipe, only leaks that can be 'sniffed' can be detected. The accuracy of above ground detection is in the order of magnitude of several meters. High pressure mains are already inspected by robotic systems. These systems are however hardly full grown autonomous robots, but more passive data loggers or PIG's. Because of the small diameter (typically 120mm or less) and the high number of obstacles, joints, bends and valves the type of gas mains in the low-pressure net is being referred to as 'un-piggable'.

C. Related research

A number of designs exist of autonomous and semi-autonomous systems for inspection of gas distribution mains, such as the Explorer by CMU [8] the MRinspect [2] and many others [6] [10] [4] [7]. Also robots exist for (visual) inspection of sewers and other pipes such as Makro[5]. None of these systems however are capable of taking a sharp mitered bend in a 63 mm pipe - which has been established as one of the key criteria for being able to operate in the given (Dutch) urban low pressure net [11]. Another requirement for this robot is a high spreading factor (maximum/minimum pipe diameter) which has to be higher than in existing robots ($125/41 = 3.05$). In this paper the design of an autonomous inspection platform will be discussed especially capable of manouvring through these small diameters and sharp bends. Besides the mere capability of moving through bends and small diameters the design is optimized and intended for long (autonomous) operation. A schematic image of the robot is given in figure 1.

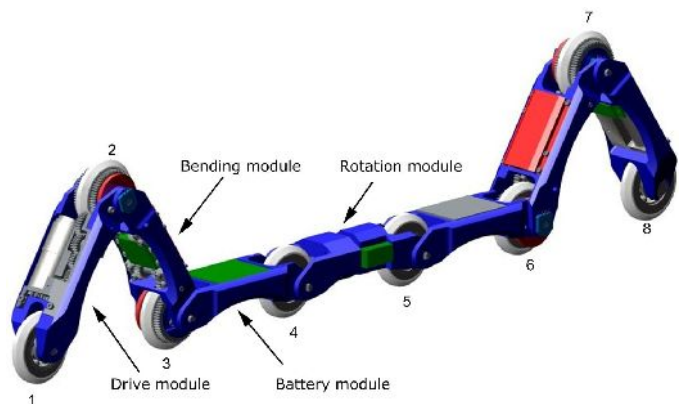


Fig. 1: Schematic drawing of the pipe inspection robot

II. REQUIREMENTS

In this section the requirements for the system will be discussed, which have led to the robot design that will be presented in the following section.

A. Goal

The final aim of this project is to realize a platform capable of autonomously inspecting a certain area of the gas distribution network, detecting leaks and recording the exact location and status of the pipe. The most stringent requirements are posed by the environment the robot has to operate in: the layout and makeup of the gas distribution network.

B. Environment

The mechanical properties of the environment regarding size and shape can be listed in order of increasing complexity for a mobile robot system and are listed in table I. The inside diameter for a pipe follows from the SDR number. Typically, SDR11 or SDR17 pipes are used. Besides the network components (arcs, bends, T-joints) the environmental temperature, moisture and contamination are also important with respect to toleration and robustness. The criteria, sizes and network elements have been selected in close cooperation with gas network operators [12] and gas distribution consultants [11].

TABLE I: Summary of Robot's environment

Property	Parametrization
straight pipe	63mm to 125 mm
inclination of the pipe	+/- 30°
gradual diameter change	63 to 125 mm, ranging from 0° to 45°
sudden diameter change by obstacle	-10 to +5 mm
deformation from outside (dent, bend)	10% increase/decrease
bends	$R \in [D/2, \rightarrow >]$
T or Y joint	choose direction[L,R]
Valves or shutters	10% diameter change
Contaminants	dust, sand, oil, water

1) *Material*: In general the robot has to move around in a PE/PVC pipe of 63 mm with a smooth surface and in a pipe of grey cast iron of 100 mm with possible corrosion. These two inner surfaces are very different. In the PE/PVC situation it is likely for the robot propulsion module to loose traction because of excessive slip due to the smooth material properties. In the case of a grey cast iron pipe, it is likely for the robot to loose traction because of contaminants (rust, dust).

2) *Connections between pipes*: Connections occur in the network with an average frequency of once per 12 m. Two methods for connecting pipes are used: by *welding* and with *sleeves*. In the PE pipe of 63 mm the welds have a height of 3 mm. In PE(125) heights of 5 mm are possible. The welds have a length varying from 6 - 11 mm. These welds, together with the allowed external deformation (dents) of the pipe, specify the maximal height and width of the robot system. In a 63 mm pipe of PE, SDR 11 (which means the wall thickness is 5.7 mm) the inner diameter is 51.5 mm. With a combined weld of 3 mm and deformation of 10% the absolute minimal diameter for the robot to pass through is 41 mm.

3) *T-joints and corners*: Although the somewhat flexible PE/PVC pipe allow (gentle) curves, normally for corners and

bends special connection pieces with varying radius (curvature) are being used. They are connected to the pipes with sleeved connection pieces. Also T joints are mostly connected with sleeves. In these T-joints and sharp 'elbow' corners we find the parts imposing the severest space- and morphological constraint on the robot design. By other systems such as the MRinspect [2], this problem has been partially solved by using T-joints and elbow joints with a smooth radius.

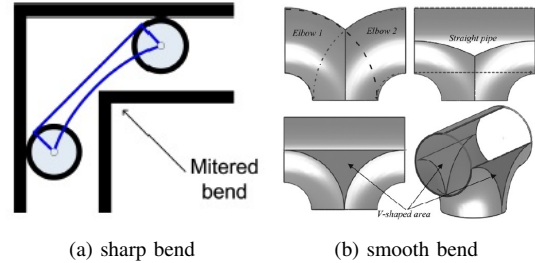


Fig. 2: Schematic drawing of robot module in sharp (mitered) bend besides a smooth bend

III. DESIGN

A. Modular Design

A modular design has been chosen for the robot system. Instead of a 'snake like' modular approach [3], the robot consists of seven modules with specific functions: two propulsion- or driving modules, two modules to clamp the robot in the tube, two payload modules and one central rotation module. The payload modules contain the power system, control electronics and sensing equipment.

As can be seen in figure 1 the robot has a symmetric layout around the central rotation module. The maximum module size is determined by the pipe diameters and obstacles as stated in table I. At least at one of the surface planes, the size of a module cannot exceed the size of the minimal pipe diameter (see figure 3) Moving through sharp elbow joints and T-joints poses another constraint, besides being able to clamp into both 63 mm and 125 mm pipes. These constraints have resulted in a curved module shape, using a wheel diameter of 40 mm and an inter-wheel distance of 90 mm.

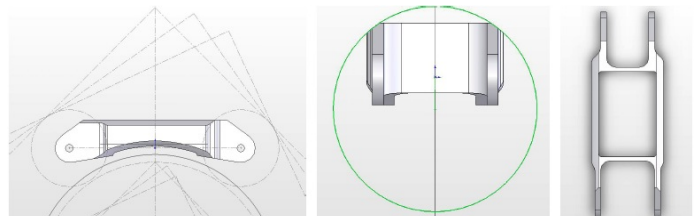


Fig. 3: Module size and shape

1) *Bending module*: The robot normally moves in the horizontal plane, in order to avoid contaminants and dust on the bottom of the pipe, as illustrated in figure 10 and 9. This means that the robot always needs to exert a certain force

on the wall in order to keep itself in the center plane of the pipe. It can generate this clamping/preloading force through a torque between the first two modules and the last two modules of the robot. Two geared motors with a spring connected acting as series elastic actuator or SEA [9] - see figure 4 - are used to generate this clamping torque. Figure 5 shows the assembly of the spring mounted inside the driven wheel. Two potentiometers are used as displacement sensors. In this configuration one of the sensors measures the angle between the modules. Since the other is connected on the same physical body, only separated by the spring, this sensor measures the spring deflection directly, independent of the angle between the modules. An other function of these motors is to bend the entire robot shape along the curve of for instance a T-joint, as shown in figure 6.

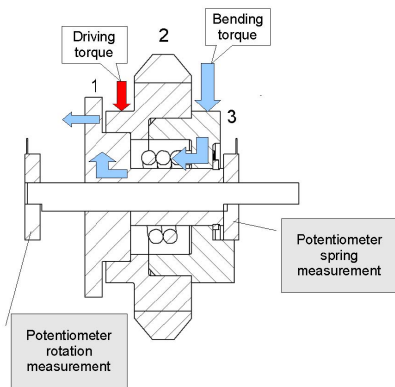


Fig. 4: Schematic drawing of series spring in wheel

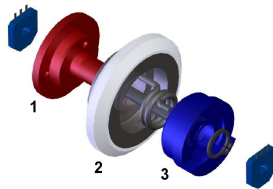


Fig. 5: Assembly drawing of spring mounted in wheel

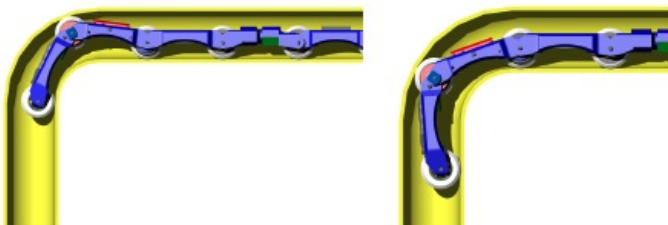


Fig. 6: Robot model in a smooth bend

A torque T is generated between the two modules and this results in a normal force on the wall, as shown in figure 7. At one side there is only one wheel. This wheel has twice the normal force of the other two wheels ($2F_n$). Because this

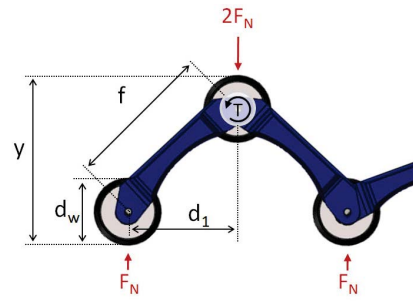


Fig. 7: Geometric relation for calculating the clamping torque

wheel has twice the normal force it is used for traction. This means that the same torque creates a larger normal force in a big pipe than in a small pipe. The driving torque also influences the preload torque: the reaction torque of the driving torque actually adds up or subtracts from the bending torque generated by the bending module $T_{preload1} = T_{bend1} + T_{drive1}$. With β the angle between the two modules:

$$\beta = \arcsin\left(\frac{d_1 - d_w}{f}\right) \quad (1)$$

using the data from table II:

$$F_n = \frac{T}{A} = \frac{T}{f \cos \beta} = 758 \text{ mNm} \quad (2)$$

The preloading torque of the bending module should be about 758 mNm in order to generate sufficient normal force. The bending actuator contains a position actuator in series with a spring, so it can be considered a torque actuator. Compliant behaviour of the bending module can compensate for small bumps and diameter changes when driving through a pipe, without using the bending actuators. A torsion spring capable

of handling the required torque appeared too large to fit in the bending module. For that reason the torsion spring is placed inside the main drive wheel. As DC motor Faulhaber 1016 has been chosen with a 1:64 gearbox. For further reduction a worm gear with a single start and a small lead angle is used. This has an additional advantage of 'self locking' behaviour. The motor does not need to be powered to maintain a certain clamping torque. The total reduction used is 1:5486, realized as shown in figure 8. Because of the use of a worm gear, the expected efficiency is very low; in the order of magnitude of 10 %.

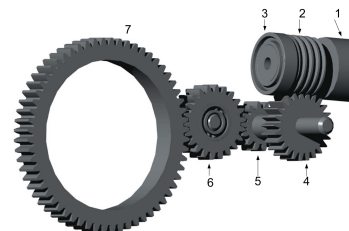


Fig. 8: Schematic drawing of gearing in bending module

2) *Traction Module*: The traction system is one of the most defining parts of the system design. Not only has the robot to move into two directions inside the pipe, also direction has to be chosen at T- and Y-junctions. Theoretically a minimum of two actuators is necessary: one for propulsion (forward and backward) and one for selection between two directions. A wide variety of propulsion mechanisms is available for in-pipe navigation, as summarized in [2]. For this system the choice has been made for wheeled propulsion since wheeled locomotion promises the best energy efficiency. Also the clamping aspect has been incorporated into the design.

The robot will drive sideways through the pipe, to avoid dust and contaminants on the bottom of the pipe. The length of the modules has been chosen such that the robot can generate a suitable clamping force in both a 125 mm pipe (119 mm inner diameter) and 63 mm (57 mm inner diameter), as shown in figures 9 and 10.



Fig. 9: Robot model in 125 mm tube

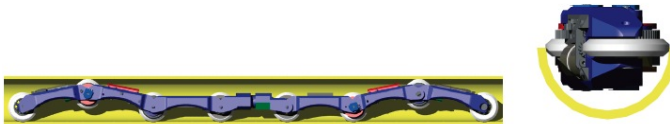


Fig. 10: Robot model in 63 mm tube

The robot has to be able to drive up a slope of 30°. Using the assumptions listed in table II the necessary torque for the used DC motor is determined.

TABLE II: Estimate values for design parameters

mass per module(m):	0.3 kg
number of module:	7
length of a module, axle to axle(L_1):	90 mm
total mass(M):	$7 \cdot 0.3 = 2.1$ kg
g:	$9.81 m/s^2$
slope(α):	30°
wheel diameter(D_1):	40 mm
pipe diameter (D_{inner}):	57 mm
friction coefficient (μ):	0.3
F_n :	normal force
F_t :	traction force

The traction force required to 'push' the robot up the slope is used for determining the necessary torque for the motors in the traction module. Not taking into account the friction due to bearings and plastic deformation of tires, the required torque for the motors is:

$$M g \sin(\alpha) \cdot \frac{D_1}{2} = 206 \text{ mNm} \quad (3)$$

with parameters are specified in table II. This torque can be divided over two motors, so each motor should deliver at least 103 mNm. A Faulhaber 1717 motor and the transmission of 1:186 yield a maximum theoretical torque at wheel of 157 mNm which is sufficiently larger than the required 103 mNm (safety factor of 1.5). The maximum driving velocity of this module is 56 mm/s. However, when performing maneuvers which require one module to unclamp (for example taking a T-joint), all necessary driving torque has to be delivered by one of the two motors. This means with the chosen configuration (157 mNm) that taking a corner cannot be executed whilst driving up a slope.

3) *Rotation module*: The motor in the rotation module should be strong enough to rotate one half of the robot with regard to the other half. When the rotating half is completely detached from the wall, it will be very easy to rotate. The motor then only has to overcome the friction in its own gearbox and the sliding bearing. If some wheels of the rotating half of the robot touch the wall, the required rotation torque has to be much larger. When during a rotation in a pipe of 119 mm one wheel touches the wall with a normal force of 10 N ($\approx 0.5 \cdot m \cdot g$) and the friction coefficient is 0.5, then the friction torque is $:(119/2) \cdot 0.5 \cdot 10 \approx 300$ mNm.

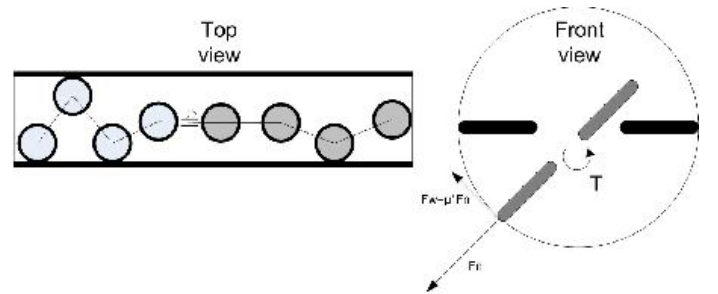


Fig. 11: Rotation torque calculation

For the rotation module a Faulhaber 1516 with a 1:809 gearbox is selected plus an incremental encoder. This combination has a maximum output torque of about 380 mNm.

B. Payload

1) *Distributed control*: Because of the modular approach of the design and the space limitations a *distributed control system* has been designed. Every joint is equipped with a small local motorcontroller, connected as 'slave' to the central 'master' controller. For communication between the main control board and the local motor control boards I²C (TWI) has been chosen with a data rate of 400 kbps.

2) *Master board*: As main control board of the robot a small controllerboard with an *LPC2148 ARM7* processor by NXP has been developed. The board fits together with a battery in one of the payload modules (see figure 12). The board communicates with a host PC system using an *Nordic NRF24L01 2.4GHz radio*, USB or 115kB serial link. Extra memory for datalogging or navigation data is added with a 1GB flash microSD card.

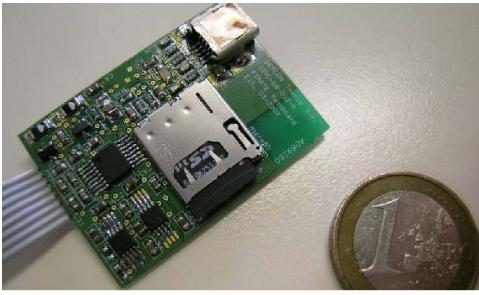


Fig. 12: Main controlboard

3) *Sensors*: On the master board a *LIS3L02 3D accelerometer* is used to determine the robots orientation with respect to the earth. Also a *TC77 spi ambient temperature sensor* for protection and monitoring of the environment is added.

4) *Power*: Switching power supply IC's convert and monitor the board's main supplies. The mainboard and motor section are powered using separate LiPo batteries in order to make the system rechargeable - and eventually energetically autonomous.

5) *Slave nodes*: Every slave on the bus consists of an 8-bit AVR RISC microcontroller and 1W H-bridge. It interfaces with local position sensors, both incremental encoders on motor-side and analog absolute position sensors on joint angles. In each slave node one or two PID controllers are implemented, running locally at 1 kHz. PID controllers can be selected to do speed, position or torque control, first ones based on position sensor information, the latter based on current measurement and position difference using the series elastic joint applying $\tau_{joint} = (\omega_1 - \omega_2)K_{spring}$. As position sensors potentiometers have been used. The slave node also monitors current consumption and protects the motors from overheating.

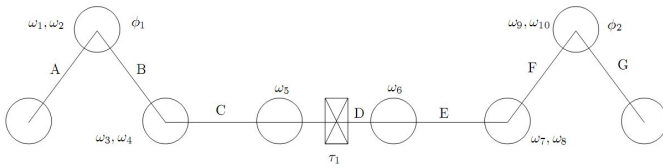


Fig. 13: Degrees of freedom for control of the robot

IV. CONTROL

The robot consists of seven segments with a total of eight wheels. Four joints are powered with the described series-elastic actuator. For each of these joints two position sensors are implemented for measuring both the positions before and after the spring $\omega_{1,2}$, $\omega_{3,4}$, $\omega_{7,8}$ and $\omega_{9,10}$ (see figure 13). The joints ω_5 and ω_6 are passive and not being controlled. Two wheels, denoted with ϕ_1 and ϕ_2 , are used for propulsion in the pipe. The rotation module angle is denoted by τ_1 .

The control software offers an interface (GUI) between the robot operator and the robot hardware. All functionality (motors, sensors) should be accesible through this interface.

Secondly the control software runs the robots statemachine for operation inside the pipe. Three levels of control are currently implemented

- 1) PID control using force (torque), position or velocity setpoints on the distributed slave controllers.
- 2) Main controller takes care of initializing, configuring and communicating with the distributed slaves.
- 3) Operator system: A PC system communicating with the robot with a GUI for scheduling motion sequences and giving direct commands.

The first two levels are implemented on the robot. An operator can manouvre the robot through the pipe by commanding *Motion Primitives*. Each robot action can be broken down to a series of these motion primitives being *clamp*, *unclamp*, *drive*, *bend*, *rotate*. For communication between the operator system and the robot both wired and wireless (2.4 GHz short range radio) have been implemented. The basic robot actions split

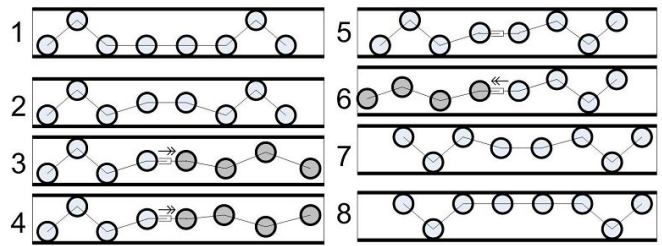


Fig. 14: Schematic drawing of axial rotation

in motion primitives:

- **drive straight**: clamp front, clamp rear, drive front, drive rear
- **axial rotation**: clamp rear, unclamp front, rotate 180°, clamp front, unclamp rear, rotate 180°, clamp rear, clamp front (see figure 14)
- **take bump**: unclamp front, drive, clamp front, drive, unclamp rear, drive, clamp rear

One of the complex maneuvers for the robot to take is the sharp (mitered) bend in a T-joint. A breakdown in motion primitives (illustrated in figure 15) can be described as follows:

- 1) clamp front ($\omega_{9,10}, \omega_{7,8}$), clamp rear ($\omega_{1,2}, \omega_{3,4}$), drive (ϕ_2, ϕ_1).
- 2) unclamp front ($\omega_{9,10}$), clamp rear ($\omega_{1,2}$), drive rear (ϕ_2), bend front ($\omega_{7,8}$)
- 3) clamp front ($\omega_{9,10}, \omega_{7,8}$)
- 4) drive (ϕ_2, ϕ_1).
- 5) bend payload ($\omega_{3,4}$)
- 6) drive (ϕ_2, ϕ_1).
- 7) unclamp rear ($\omega_{1,2}, \omega_{3,4}$)
- 8) unbend payload module ($\omega_{3,4}$)
- 9) clamp rear ($\omega_{1,2}, \omega_{3,4}$), continue to drive (ϕ_2, ϕ_1).

V. RESULTS

The robot has been put through a series of preliminary experiments, testing the driving capabilities, joint control and

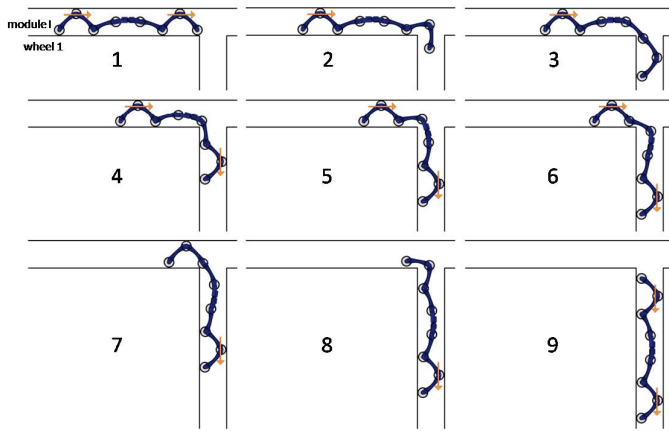


Fig. 15: Schematic overview of robot moving through sharp corner

overall control. The robot can maneuver through pipes with different diameter, drive under angles of 30° and rotate around its central axis. The robot can move forward with a velocity of 5.6 cm/sec. Torque control of the clamping modules has been implemented using current control. In the image sequence displayed in figure 16 the robot successfully negotiates a sharp (mitered) bend in a 90 mm tube. These tests were conducted with wired power supply and communication cable, which will be replaced by batteries and (when not operating autonomously) short range radio link in the future.

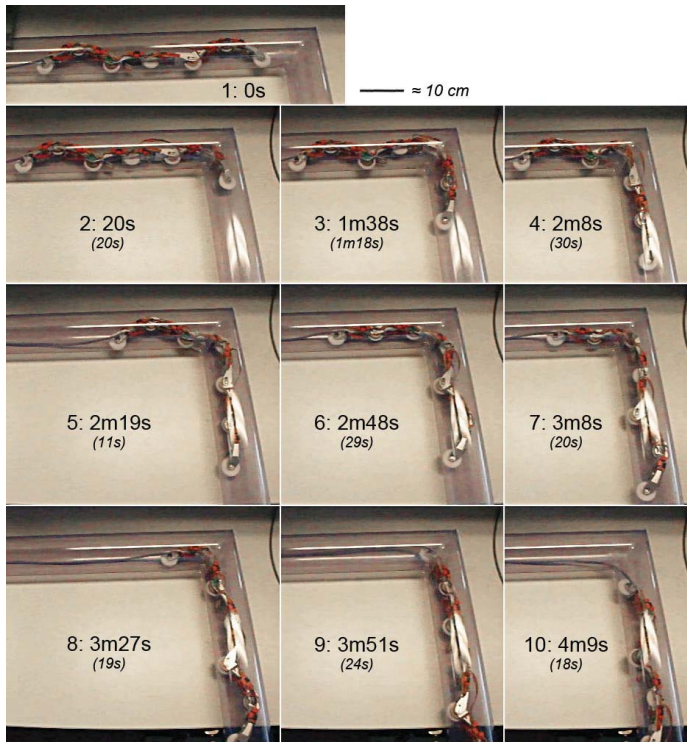


Fig. 16: Robot moving through a sharp corner

VI. CONCLUSIONS

A. System design

The robot is capable performing the desired maneuvers, showing the most complex (negotiating a sharp bend) in figure 16. The velocity (5.6 cm/sec) and clamping control prove satisfactory regarding both the design and the chosen components (motors, gears). The robots mechanical setup provides an suitable test bed for further development of sensors and navigation software.

B. Ongoing work

At the moment the current design is being tested in a test-track consisting of a wide variety of materials and a large selections of bends and joints. In situations (bends, junctions) when only one motor can be used for propulsion, the amount of available torque might not be sufficient under all conditions. One of the solutions would be to increase the number of traction+bend modules to three (so three V-shaped clamps), which is currently under investigation.

An optical sensor system for obstacle detection and pipe characterization is under development. The output of this sensor, combined with IMU- and odometric data, is being used in a system for simultaneously localization and mapping (SLAM) in the network.

REFERENCES

- [1] Pulles, C.; Dertien, E.C.; Pol, H.J. van der; Nispeling, R.; *Pirate, the development of autonomous gas distribution system inspection robot*, IGRC 2008 - October 8-10, 2008
- [2] Roh, S. and Choi, H.R., *Differential-Drive In-Pipe Robot for Moving Inside Urban Gas Pipelines*, IEEE Transactions on Robotics, vol. 21, no. 1, february 2005
- [3] Suzumori, K.; Wakimoto, S.; Takata, M.; *A miniature inspection robot negotiating pipes of widely varying diameter*, Robotics and Automation, 2003. Proceedings. ICRA '03. IEEE International Conference on , vol.2, no., pp. 2735- 2740 vol.2, 14-19 Sept. 2003
- [4] E.Gambao, M. Hernando and A. Brunete, *Multiconfigurable Inspection Robots for Low Diameter Canalizations*, ISARC 2005 - September 11-14, 2005
- [5] Streich, H.; Adria, O.; *Software approach for the autonomous inspection robot MAKRO*, Proc of the 2004 IEEE International Conference on Robotics and Automation, pp. 3411 - 3416 Vol.4
- [6] Foster-Miller, *Development of an Inspection Platform and a Suite of Sensors for Assessing Corrosion an Mechanical Damage on Unpigable Transmission Mains*, NGA and Foster-Miller, March 2004.
- [7] Hirose, S.; Ohno, H.; Mitsui, T.; Suyama, K. *Design of in-pipe inspection vehicles for $\phi 25$, $\phi 50$, $\phi 150$ pipes*, Proc. ICRA 1999. pp. 2309 - 2314 vol.3
- [8] Schempf, Hagen and Mutschler, Edward and Gavaert, Alan and Skoptsov, George and Crowley, William. *Visual and nondestructive evaluation inspection of live gas mains using the ExplorerTM family of pipe robots*, Journal of Field Robotics, vol 27, no 3, pp. 217-249, 2010.
- [9] Pratt G and Williamson M, *Series Elastic Actuators*. Proceedings of the IEEE International Conference on Intelligent Robots and Systems 1: 399-406, 1995.
- [10] Anouar Jamoussi, *Robotic NDE: A New Solution for In-line Pipe Inspection*, 3rd MENDT - Middle East Nondestructive Testing Conference And Exhibition - 27-30 Nov 2005 Bahrain, Manama
- [11] Pulles, K, *Requirements for robot inspection of gas distribution mains*, Internal report, KIWA Gas Tec, 2006
- [12] <http://www.alliander.nl>